

Numerical study of performance of soil-steel bridge during soil backfilling

Damian Beben*

Faculty of Civil Engineering, Opole University of Technology, Katowicka Street 48,
45-061 Opole, Poland

(Received November 16, 2010, Revised January 25, 2012, Accepted April 24, 2012)

Abstract. This paper presents results of a numerical analysis performed on a corrugated steel plate (CSP) bridge during a backfilling process. The analysed bridge structure was a box culvert having a span of 12315 mm as well as a clear height of 3550 mm. Obtained calculation results were compared with the experimental ones. The paper is presented with the application of the Fast Lagrangian Analysis of Continua (FLAC) program based on the finite differences method (FDM) to determine behaviour of the soil-steel bridge structure during backfilling. The assumptions of a computational 2D model of soil-steel structure with a non-linear *interface* layer are described. Parametric analysis of the interface element is also given in order to receive the most realistic calculation results. The method based on this computational model may be used with large success to design calculations of this specific type of structure instead of the conventional and fairly inaccurate analytical methods. The conclusions drawn from such analysis can be helpful mostly for the assessment of the behaviour of steel-soil bridge structures under loads of backfilling. In consideration of an even more frequent application of this type of structure, conclusions from the conducted analysis can be generalized to a whole class of similar structural bridge solutions.

Keywords: soil-structure interactions; soil-steel bridge; steel corrugated plate; finite difference method; backfilling

1. Introduction

The subject of numerical study was a single-span road bridge made from corrugated steel plate (CSP) elements (Fig. 1(a)). The field load tests and the initial calculations of this structure were conducted in three various stages which were thoroughly described in papers (Manko and Beben 2005c, 2008).

The specific nature of soil-steel bridges depends on the fact that they consist of two entirely different media (soil and steel), and therefore the whole load bearing system becomes flexible (AASHTO 2002, Beben 2005, McGrath *et al.* 2002, Pettersson and Sundquist 2007, Vaslestad 1990). Thanks to the interaction between these component units, i.e., their mutual influence, a “combined” load-carrying system is formed. The structural system also allows the transfer of external loads considerably larger than in the case of treating the CSP shell as the main load bearing system in such bridges because it does not cause increased stresses and displacements in them.

*Corresponding author, Ph.D., E-mail: d.beben@po.opole.pl

Static and dynamic analyses of soil-steel bridges are presented in many works. A special manner of dynamic analysis of a buried structure was presented by Dancygier and Karinski (2000). Moreover, the application of the Single Degree Of Freedom (SDOF) model to simulate wave propagation at the buried structure was shown. The mathematical formulation and solution of the applied model were also described. The stress distributions around underground structures are presented in the paper written by Karinski *et al.* (2009). The analysis was performed utilizing the Boundary Integral Equation (BIE) method coupled with the Neumann series. The damage assessment method for buried structures against special dynamic impact (an internal blast) considering the soil-structure interaction was presented by Ma *et al.* (2009). A case study for a buried structure has been conducted to show the applicability of the proposed damage assessment method. Hernandez-Montes *et al.* (2005) propose the use of underground arches to support gravity loads, wherein the horizontal thrust of the arch is equilibrated by soil pressure. Because the horizontal soil pressure increases with depth, the depth of the arch may be reduced as the depth below grade increases. Beben (2009) presents calculations of the steel culvert using the finite differences method mainly in the range of static loads.

The large load-carrying capacity of such structures has been shown many times during experimental tests (Arockiasamy *et al.* 2007, Beben 2005, Beben and Manko 2010, Flaner and Karoumi 2009, Flaner *et al.* 2005, Manko and Beben 2005a, b, c, 2008, Sargand *et al.* 2008, Sazen *et al.* 2009, Vaslestad 1990, Yeau *et al.* 2009). It results from the interaction of two media but at the same time it is difficult to formulate and estimate in a traditional (analytical) computational way. The correct description of this specific structural system requires searching for special ways of analyzing of such objects (Kang *et al.* 2008, Kim and Yoo 2005, Rotter and Jumikis 1998).

The calculations presented in this study were executed with the Fast Lagrangian Analysis of Continua (FLAC) program based on the finite differences method (FDM), with the *interface* elements (contact layers) occurring on the contact point of two media. The FDM allows the solving of various problems concerning the structural mechanics and geomechanics for several different media, which makes possible, among other things, defining the load-carrying capacity of such bridges.

The main goal of the complex FDM analysis on this bridge was to determine the displacements, strains (normal stresses) and bending moments of the structure during the backfilling process. The behaviour of geotechnical structures such as soil-steel bridges is strongly influenced by the soil-structure interaction. The correct description of interface elements was received on the base of the parametric study.

The comprehensive and thorough analyses of displacements, strains (normal stresses) and bending moments, and the conclusions drawn from such analyses can be useful in engineering practice, particularly in the calculations of soil-steel bridges instead of the conventional and fairly inaccurate analytical methods. This study may also be used for developing design and acceptance guidelines concerning such structures.

Detailed descriptions of an analysed soil-steel bridge and instrumentation of field load tests (load schemes, arrangement of gages, equipments, measurement accuracy, errors, etc.) were presented in papers written by Manko and Beben (2005a, b, c).

2. Conventional design methods

The most current design methods consider pure ring compression as their main design criteria.

Ring compression forces are most applicable and most important in cases of structures with high covers. However, as the span increases or soil cover decreases; bending moments, displacements and stresses become more significant design considerations. For the soil-steel structures (e.g., pipes, culverts, bridges), three main design criteria are usually used:

1. The deflection criteria. The most commonly used deflection equation is the well-known Iowa formula, developed by Spangler and Martson for computing the change in the horizontal diameter of flexible steel (or plastic) culverts. This formula consists of the controversial modulus of soil reaction. Spangler postulated that pressures distributions are proportional to movement (Vaslestad 1990). The assumption of the Iowa deflection formula may be summarized as follows:
 - the vertical load is distributed uniformly over the width of the structure;
 - the reaction on the bottom of the structure is equal to the vertical load and is distributed uniformly over the bedding of the structure;
 - the horizontal pressure is distributed parabolically over the middle 100° of the structure and the max unit pressure is a result of the modulus of passive resistance and 1/2 of the horizontal deflection of the structure.
2. The thrust criteria – compression loads for the structure wall. The thrust is limited to a value that will not cause seam failure or wall material yielding. The ring compression theory is used. This theory states that the structure wall should be designed to resist the compression stresses and deflections produced by a hydrostatic soil pressure equal in magnitude to the overburden pressure. The distribution of soil pressure according to the ring compression theory was developed by White and Layer for the different shapes (Beben 2005).
3. The buckling criteria. Elastic buckling originates as a local bugle and may occur at the crown or at other locations, depending on where the critical combination of force, bending moment imperfection and residual stresses first develops (Beben 2005, Vaslestad 1990).

On the basis of the above-mentioned conventional design criteria, various methods and programs were developed, e.g.: the AISI method, the ASTM method, the AASHTO method, the ARMTEC super-span method, the CANDE program, the SCI method, the UBC culvert design procedure (an improvement of the SCI method), the OHBDC method, the CHBDC method, the Vaslestad method and the Sundquist-Pettersson method (Beben 2009).

The above-mentioned conventional methods are very conservative. The calculations of the soil-steel bridge structures used by such methods are incorrect in comparison with the results received from the experimental tests. This probably results from the versatility of such methods as well as simplifications being too large (Beben 2005, Vaslestad 1990).

For the most part, current design methods for the soil-steel bridge structures are based on experience rather than a viable analytical model. This is because a reasonable analytical model is quite complicated. These complications are due to the interaction phenomena. In such composite systems, both the soil and steel structures are required to be taken into consideration as the load-carrying elements, and it isn't possible simply to accept only as the loads acting on the structure (Beben 2005).

Up to now, the calculation results obtained by use of the computational models in comparison with the experimental results are insufficiently satisfactory. Kunecki (2006) used the Drucker-Prager elastic-perfectly plastic soil model. The FEM results were higher than the ones received from field tests. El-Sawy (2003) used the isoparametric brick elements for soil modelling. FEM and test results indicate that this soil model is insufficient. Taleb and Moore (1999) executed two-

dimensional FE analysis while using the Coulomb-Mohr model. The results were also in the low accuracy level in comparison to experimental tests. Machelski and Antoniszyn (2004) and Machelski *et al.* (2006) used isotropic elements (PLANE2D) to model the soil media. Their predictions were also too large in relation to the test results. The initial calculations of the soil-steel bridge using the Coulomb-Mohr soil model were presented by Beben (2009). For the above reasons, the material properties (soil, steel structure and contact layers) should be assumed as the most real.

3. Model of the soil-steel bridge with interface elements

3.1 General notes

The calculations (and experimental tests) were performed in three cross sections along the length of the shell structure under backfill loads during the soil compaction around the structure, and were carried out six times for different numbers of layers (Fig. 1(a)). The horizontal and vertical

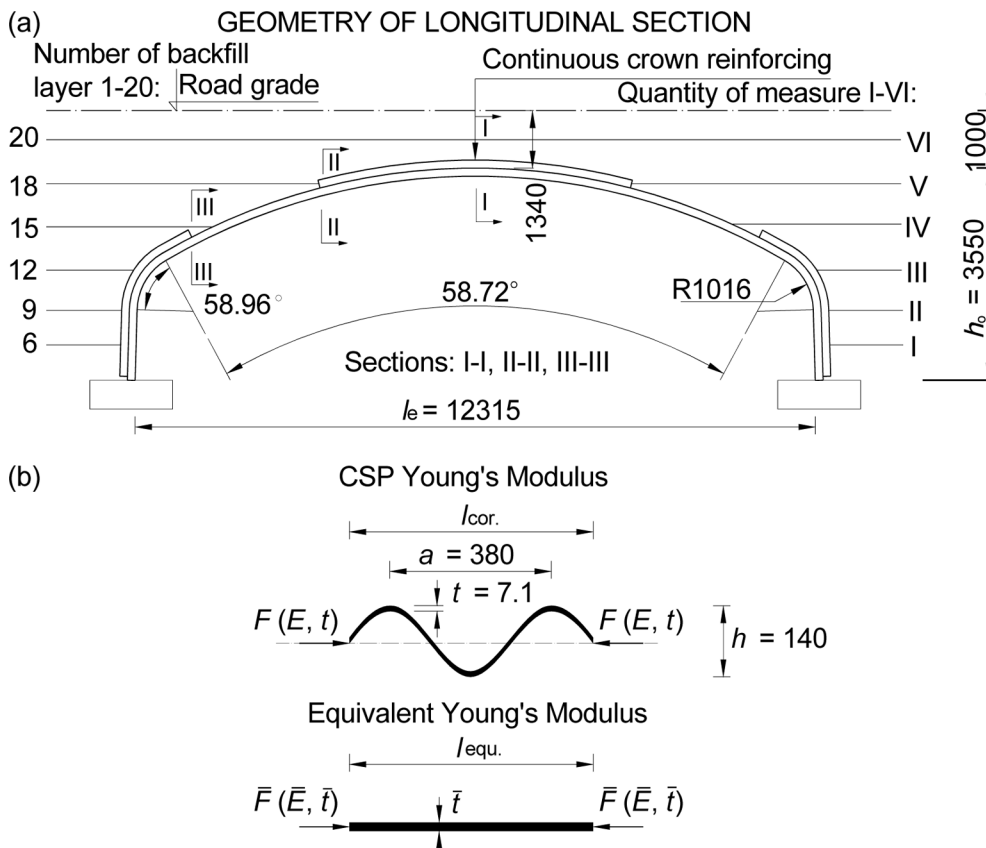


Fig. 1 (a) The geometry of longitudinal section of the CSP structure, (b) corrugation detail and equivalent Young's modulus

displacements as well as strains (normal stress indirectly) in the longitudinal and transversal shell direction in three examined sections were calculated (and tested on a real object), i.e. in the crown (cross section I-I), at the end of shell reinforcing (cross section II-II), and in its haunches (cross section III-III) (Manko and Beben 2005a, c).

The initial analytical computations were conducted by Manko and Beben (2005a, c) and the received results in comparison with the experimental ones were not very accurate. Therefore, a decision was made to look for new ways of calculations using the real material properties as well as taking into account the non-linear contact elements of interface type. The constitutive modelling of the soil-structure interfaces plays a major role in the numerical simulation of the soil-structure interaction problem (Hu and Pu 2003). It follows from the above that other numerical methods should be sought and assumptions that are more realistic should be made during creation of the computational models of such soil-steel bridge structures.

The computations of the soil-steel bridge were conducted using the *FLAC* 2D program (ver. 3.4), which permits of the realization of the selected problems concerning statics and dynamics of the structure for the plane soil-steel systems. For the FDM analysis (2D computation model – Fig. 2(a)) the following mesh was used:

- rectangular mesh to represent the CSP structure;
- rectangular (locally triangular) mesh to represent the backfill;
- non-linear interface elements to connect the CSP structure and the soil medium (backfill).

The soil was modelled as the hyperbolic stress-strain relationship (Duncan-Chang model) (Duncan and Chang 1970). Non-linear soil behaviour was approximated by incremental analyses; i.e., by changing soil properties as backfill was placed and compacted. Values of tangent modulus and Poisson's ratio were computed for each layer based on the assumption that vertical and horizontal soil stresses are principal stresses (Kang *et al.* 2005). Modulus variation $E(z)_{soil} = E_{osoil} + m_{soil}z$ is defined using the surface modulus E_{osoil} and the modulus gradient m_{soil} on the depth z . Two soil densities were used to model various soil zones (Fig. 2(a)). For first soil density, i.e. 95% (type A)

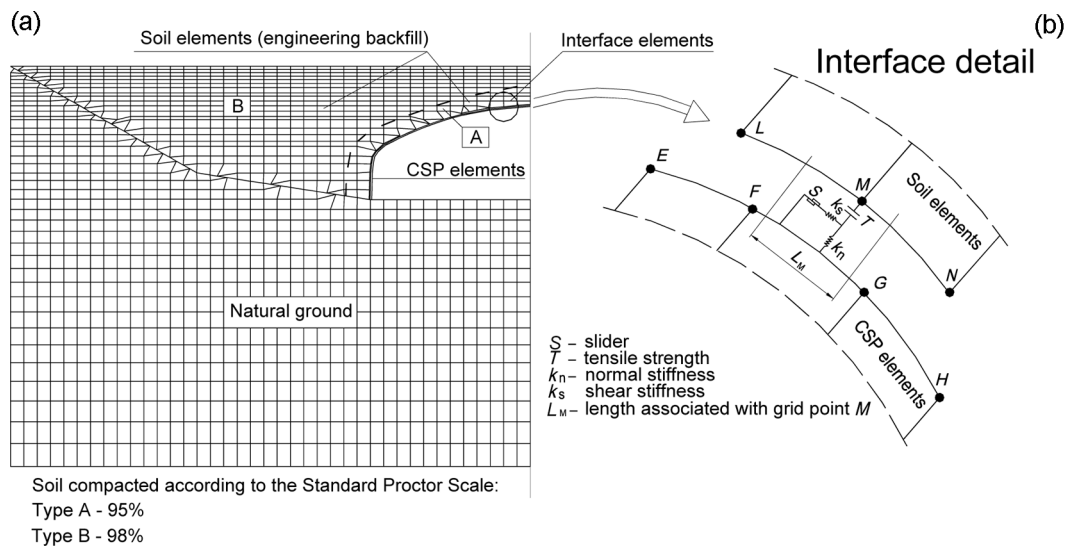


Fig. 2 Model of soil-steel bridge: (a) finite differences mesh, (b) interface detail

and second (98% – type B) according to the Normal Proctor scale, the following parameters were applied: the Poisson's ratio $\nu_{soil} = 0.20$ (0.0); the cohesion $c_{soil} = 0.0$ (0.0), the friction angle $\phi_{soil} = 43^\circ$ (35°); the gradient $m_{soil} = 3.8$ MPa/m; $E_{soil} = 20$ MPa, the unit weight of soil $\gamma_{soil} = 20$ kN/m³, the dilation angle $\psi_{soil} = 0.0^\circ$ (0.0°) and the failure ratio $R_{fsoil} = 0.95$ (0.85). The soil parameters were received from the lab tests. Analyses were carried out as class "C1" predictions (Lambe 1973), which are categorized as cases where the actual results are available at the time of the analyses. In this case, the analysis should be described as "back-analysis".

The CSP structure was modelled as bilinear elastic with material constants of: the initial Young's modulus $E_{1s} = 207$ GPa; the secondary Young's modulus $E_{2s} = 79.6$ GPa; the Poisson's ratio $\nu_s = 0.30$; the yield stress $\sigma_{ys} = 300$ MPa; the plate thickness $t_s = 7.10 \times 10^{-3}$ m; the moment of inertia $I_s = 2.07 \times 10^{-5}$ m⁴/m and the cross-sectional area $A_s = 8.40 \times 10^{-3}$ m²/m. The CSP parameters were received from the producer of these structures.

To model the axial and bending stiffness and material properties of the CSP in the circumferential direction (Fig. 1(b)), the equivalent circumferential Young's modulus \bar{E}_s and shell thickness \bar{t}_s were calculated based on the following Eqs. (1) and (2)

$$\bar{E}_s = \frac{12E_{1s}I_s}{\bar{t}_s^3} \quad (1)$$

$$\bar{t}_s = \sqrt{\frac{12I_s}{A_s}} \quad (2)$$

where E_{1s} is the Young's modulus of steel, A_s and I_s are the area and moment of inertial of the unit width of the corrugated plate (with thickness t_s), measured in the circumferential direction, respectively.

The concrete footings were modelled as elastic. The elastic modulus $E = 30$ GPa and Poisson's ratio $\nu = 0.17$ were applied.

The computation analysis was executed in the range of non-linear statics with use of the non-linear hyperbolic interface elements. The loads in the form of backfill layers evenly spread on a width of 1.00 m were applied. The thickness of backfill layers amounted to 0.20 m. The vibratory plates were used for soil compaction during construction. The measurements were carried out after compaction of each of the analysed backfill layers. Therefore, the direct impact of forces coming from the vibration plates has been omitted in calculations. The FDM calculations were conducted four times (for various interface types) for 6 selected numbers of backfill, which corresponded with layers (6, 9, 12, 15, 18 and 20), for which the experimental field load tests were also executed (Manko and Beben 2005c).

The two-dimensional analyses were performed step by step, beginning with the structure resting on its foundation without backfills. The placement of the first layer of backfill alongside the culvert was modelled by adding the first layer of soil elements to the finite difference mesh. At the same time, loads were applied representing the weights of the added soil elements. Through their interaction, the shell structure was loaded by the soil elements. Subsequent steps of the analyses were performed in the same way, adding one layer of elements at a time, which simulates the process of backfilling around and over the shell structure.

After the final layer of backfill had been placed over the top of the structure, loads were applied to the surface of the fill to simulate vehicular traffic loads (Beben 2009).

3.2 Interface contact elements

There are several instances in geomechanics in which it is desirable to represent planes on which sliding or separation can occur. The additionally specific interface elements on the point of contact of different materials were applied to formulate these problems.

The formulation the growth of structure response facilitates modelling the non-linear behaviours, such as the characteristics of soil and structure: the stress-strain ($\sigma - \varepsilon$) as well as interaction of the steel shell-soil system with regard to the contact layer on the point of contact of both materials. One should provide interface elements that are characterized by Coulomb sliding and/or tensile separation. The simulation of contact interface between soil and structure by using the Mohr-Coulomb friction concept was presented by Nagy *et al.* (2010).

Interfaces have the properties of friction, cohesion, dilation, normal and shear stiffness, and tensile strength. Although there is no restriction on the number of interfaces or the complexity of their intersections, it is generally not reasonable to model more than a few simple interfaces with the *FLAC* program because it is awkward to specify complicated interface geometry.

An interface element is represented as a normal (k_n) and shear stiffness (k_s) between two planes (e.g., soil and steel), which may contact one another, as shown on Fig. 2(b). For its description it uses contact logic for either side of the interface which is similar in nature to that which is employed in the distinct element method. The distinct element method is a theory proposed by Cundall and Hart (1992). In this method, any particle that exists is regarded as a rigid element, and the behaviour of this element is expressed by an equation of motion of mass point. A spring is provided between rigid elements which make contact with each other so as to express the interaction of force between them. Then, the equation of motion of each rigid element is solved and the solution is subjected to numerical integration on a time axis, whereby the behaviour of the element is analysed.

In order to receive the most real interaction between the soil and the CSP structure, the parametric study of the interface elements was made. The non-linear hyperbolic interface element properties used for parameterization are shown in Table 1.

The code keeps a list of the grid points (i, j) that lie on each side of any particular surface. Each point was taken, in turn, and checked for contact with its closest neighbouring point on the opposite side of the interface element. According to Fig. 2(b) grid point M is checked for contact on the segment between F and G . If contact was detected, the normal, k_n , to the contact, M , was computed,

Table 1 The composition of the four various interface element properties used to the parametric study

Interface properties	Interface type			
	I	II	III	IV
Normal stiffness $k_{n \text{ int}}$ (kN m ⁻³)	2.0×10^8	2.6×10^8	3.5×10^8	4.0×10^8
Shear stiffness $k_{s \text{ int}}$ (kN m ⁻³)	1.5×10^6	1.8×10^6	2.0×10^6	2.2×10^6
Friction angle ϕ_{int} (°)	25	30	35	40
Cohesive strength c_{int} (kPa)	0.80	1.00	1.20	1.40
Failure ratio $R_{f \text{ int}}$	0.80	0.85	0.90	0.95
Tensile strength T_{int} (MPa)	0.10	0.00	0.15	0.20

and a “length” L_{int} , defined for the contact along the interface belonging to M , where L_{int} was equalled to half the distance to the nearest grid point to the left plus half the distance to the nearest grid point to the right, irrespective of whether the neighbouring grid point was on the same side of the interface or on the opposite side. In this way, the entire joint was divided into contiguous segments, each controlled by a grid point.

During each time step $t + \Delta t$, the velocity, \dot{u}_i , of each grid point was determined. Since the units of velocity are displacement per time step and the calculation time step has been scaled to unity to speed convergence, then the incremental displacement for any given time step was amounted $\Delta u_i \equiv \dot{u}_i$. Next the incremental relative displacement vector at the contact point was resolved into the normal and shear directions, and total normal and shear forces were determined by Eqs. (3) and (4)

$$F_n^{(t+\Delta t)} = F_n^{(t)} - k_{n \text{ int}} \Delta u_n^{(t+\frac{1}{2}\Delta t)} L_{\text{int}} \quad (3)$$

$$F_s^{(t+\Delta t)} = F_s^{(t)} - k_{s \text{ int}} \Delta u_s^{(t+\frac{1}{2}\Delta t)} L_{\text{int}} \quad (4)$$

where $F_n^{(t+\Delta t)}$ – total normal force at time $(t + \Delta t)$, kNm; $F_s^{(t+\Delta t)}$ – total shear force at time $(t + \Delta t)$, kNm; $k_{n \text{ int}}$ – the normal stiffness, kNm^{-3} ; $k_{s \text{ int}}$ – the shear stiffness, kNm^{-3} ; Δu_n – incremental relative normal displacement, m ; Δu_s – incremental relative shear displacement, m ; L_{int} – effective contact length, m .

Next the Coulomb shear-strength criterion limits the shear force by the relation (5)

$$F_{s \text{ max}} = c_{\text{int}} L_{\text{int}} + tg\phi_{\text{int}} F_n \quad (5)$$

where $F_{s \text{ max}}$ – Coulomb shear-strength criterion limits for the shear force, kNm; c_{int} – cohesion along the interface, kPa; L_{int} – effective contact length (Fig. 2(b)), m ; ϕ_{int} – friction angle of interface surfaces, ($^\circ$); F_n – total normal force, kNm.

4. Calculation results

The FDM calculations of the soil-steel bridge were made for four various interface element types. As a result of the parametric study, the second applied interface type (II) was estimated as the most real. The relative variations of displacement and strain for the second interface type were the smallest, which means that they were most similar to the experimental ones (Fig. 3).

The selected values of displacements, normal stresses (strains) and bending moments in the three cross sections of the shell obtained from the FDM analysis are presented in Figs. 4, 5 and 6. The presented calculation results were made for above-mentioned soil and steel parameters as well as for the second kind of interface (II); whereas, the comparison of maximal values obtained from numerical calculations and experimental tests are presented in Figs. 7 and 8.

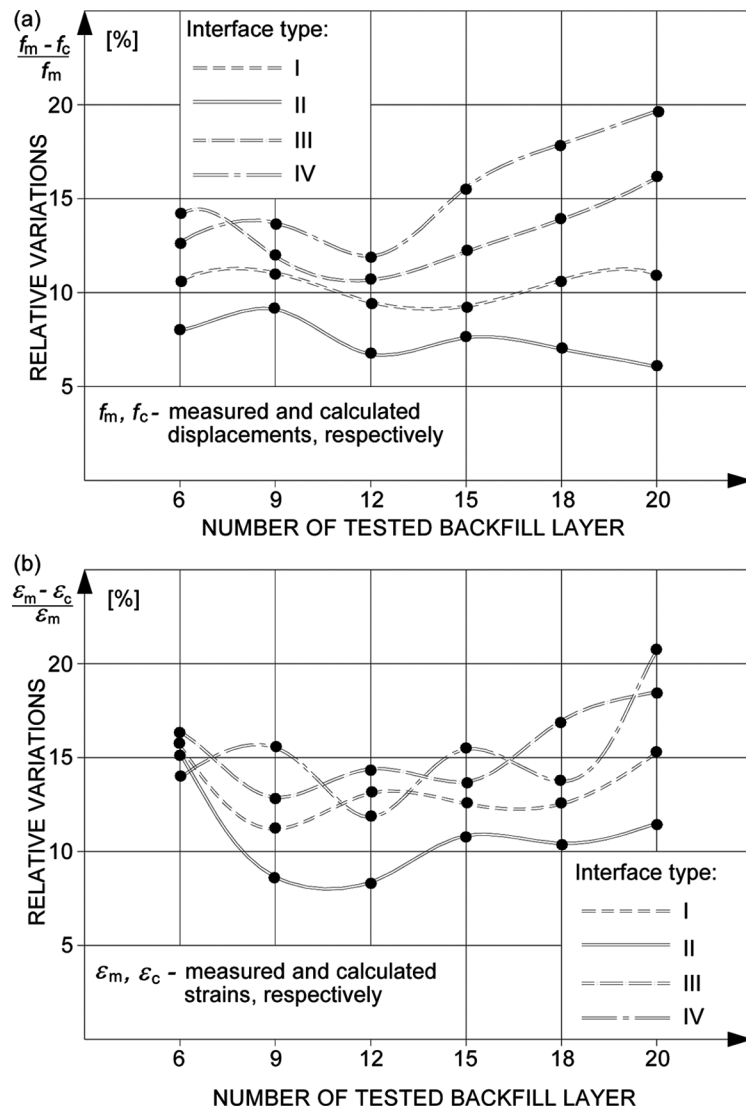


Fig. 3 The courses of relative variations of vertical displacements (a) and strains (b), received from FDM calculations for four various interface elements

5. Analysis of results obtained from calculations and tests

5.1 General remarks

The analysis of the displacements and normal stresses received from FDM calculations in three selected sections of the shell structure made from the CSP demonstrated that they were mostly higher than the measured values in the same sections. As shown in Fig. 7, the relationship between displacements (strains) and number of tested backfill layer is strongly non-linear. Therefore the assumption that the soil and interface were modelled as non-linear seems correct.

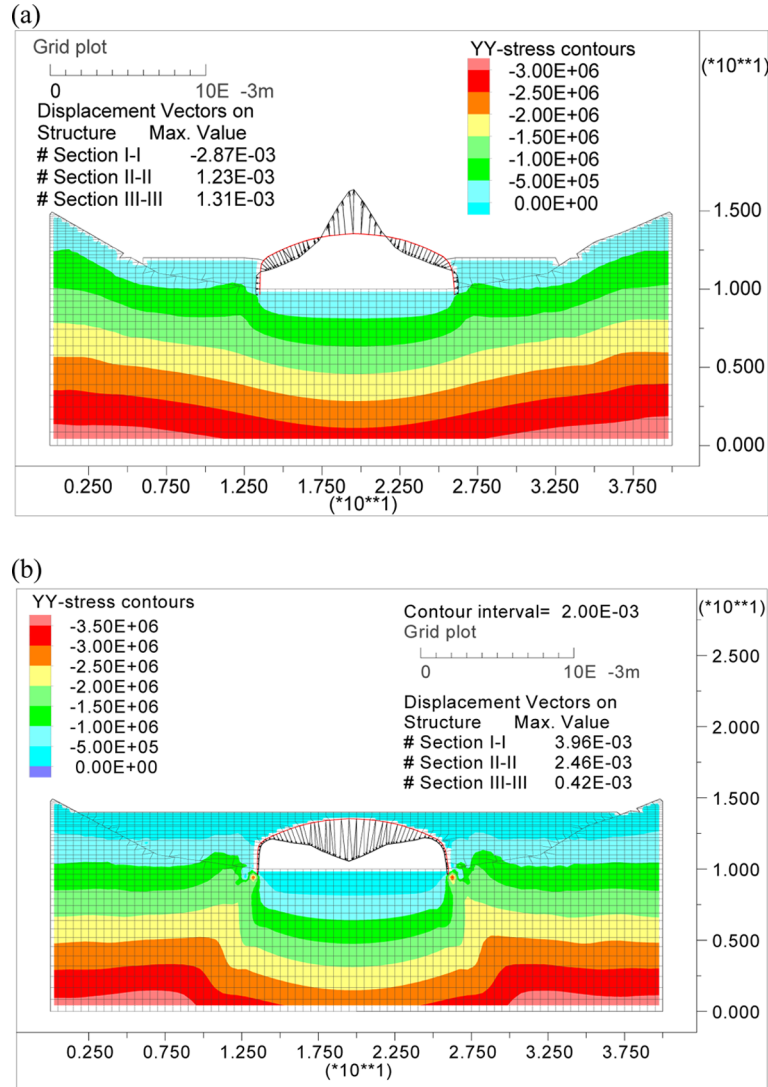


Fig. 4 Graphs of selected vertical displacements in steel shell structure obtained from backfilling and compacting of soil layers: (a) 15 and (b) 20

The analysis of results conducted at this stage of the research was very crucial, because, among other things, the steel structure of the shell was for the first time loaded by the pressure of backfill. In the results of the thorough analysis of displacements and strains, strength and behaviour of the thin walled steel shell structure were determined; and the first stage of interaction between soil and a component element was estimated.

5.2 Vertical and horizontal displacements

The highest vertical displacements in the shell structure made from the CSP in the section I-I (crown) were obtained from computation after the final compaction of the 20th soil layer. They

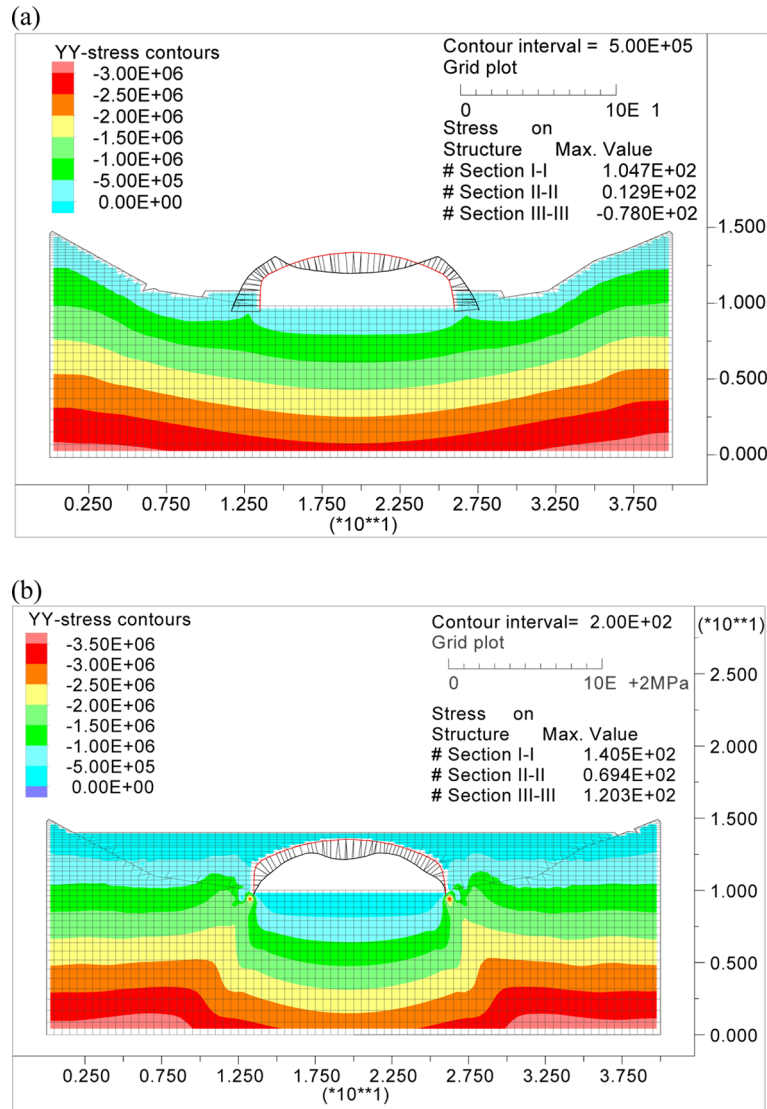


Fig. 5 Graphs of selected normal stresses in steel shell structure obtained from backfilling and compacting of soil layers: (a) 9 and (b) 20

amounted to $f_{vc} = 3.96 \times 10^{-3}$ m and they were concentrated in the middle of the shell width (Fig. 4(b)). At the same point, the measured value equalled $f_{vm} = 3.72 \times 10^{-3}$ m. In the section II-II the maximum vertical displacements of the load bearing structure amounted to $f_{vc} = 2.46 \times 10^{-3}$ m; they also occurred during the compaction of the 20th soil layer (Fig. 4(b)). In this case, the measured value amounted to $f_{vm} = 2.62 \times 10^{-3}$ m. In the section III-III the maximum vertical displacements of the steel shell structure amounted to $f_{vc} = 1.31 \times 10^{-3}$ m and they occurred after the 15th soil layer compaction (Fig. 4(a)). The measured value equalled $f_{vm} = 1.17 \times 10^{-3}$ m.

In the three analyzed sections (I-I, II-II and III-III), maximum horizontal displacements obtained from calculations and measurements did not exceed $f_{hc}, f_{hm} < 0.53 \times 10^{-3}$ m.

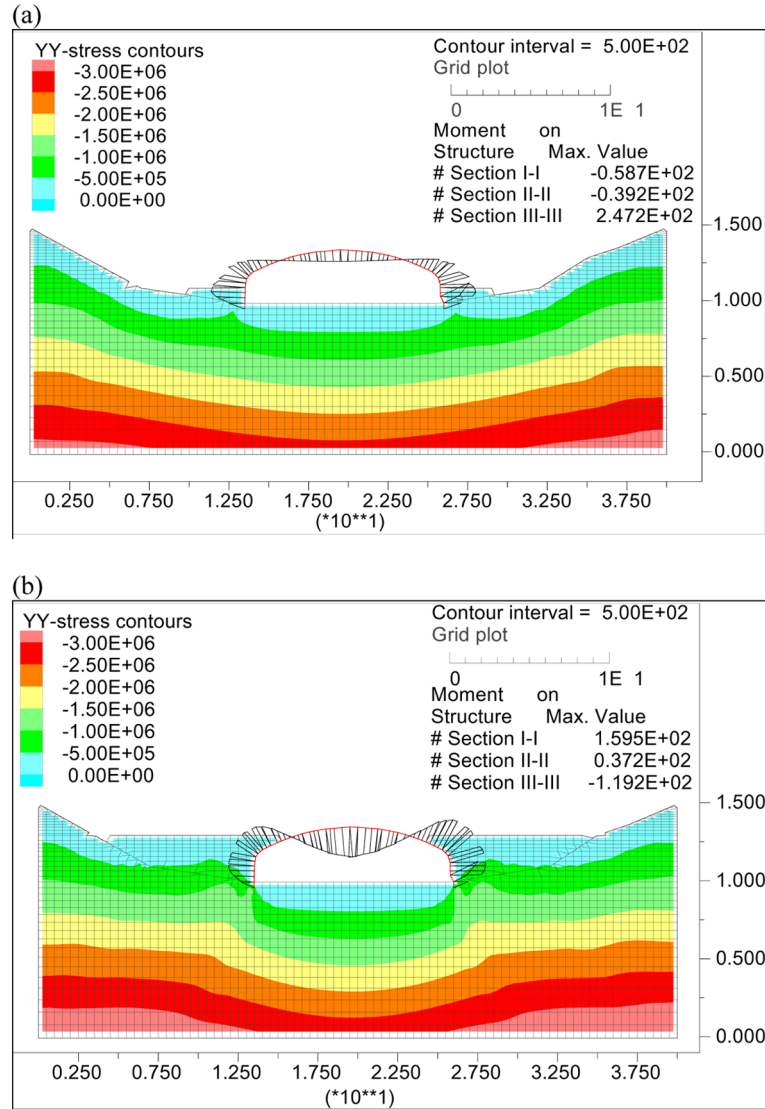


Fig. 6 Graphs of selected bending moments in steel shell structure obtained from backfilling and compacting of soil layers: (a) 9 and (b) 18

During the compaction of the first layers (nos. 6, 9 and 12), the shell crown moved upwards – the change of sign of displacements (Fig. 8(a)) and the shell lateral walls near the foundation moved inwards. During compaction of the subsequent backfill layers (nos. 15, 18 and 20), the side elements of the shell structure began to move toward the soil and the upper part (crown) moved downwards (Fig. 8(a)).

5.3 Strains (normal stresses)

The highest strains (normal stresses) in the steel shell structure obtained from the calculations

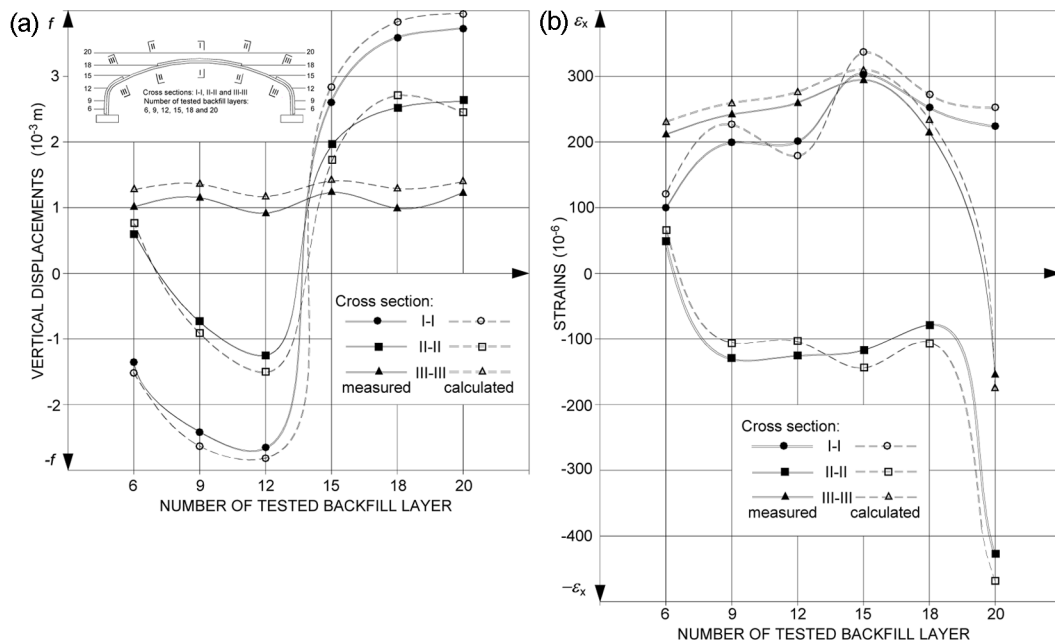


Fig. 7 Comparison of measured and calculated values of vertical displacements (a) and strains (b) in time of backfilling process in three cross sections I-I, II-II and III-III

occurred in the section I-I, i.e. in the crown of the shell, during the compaction of the 20th backfill layer, and their maximum value amounted to $\varepsilon_{yc} = 679 \times 10^{-6}$ ($\sigma_{yc} = 140.5$ MPa). They occurred in the top of corrugations in the transversal direction of the structure (Fig. 5(b)). The measured value of strain (normal stresses) equalled $\varepsilon_{ym} = 648 \times 10^{-6}$ ($\sigma_{ym} = 134.1$ MPa).

In the next analysed section II-II, the highest strains (normal stresses) calculated in the transversal direction of the shell structure occurred during the compaction of the 20th backfill layer, and their value amounted to $\varepsilon_{yc} = 555 \times 10^{-6}$ ($\sigma_{yc} = 114.9$ MPa) and manifested itself in the bottom of corrugations. At the same point, the measured strain value amounted to $\varepsilon_{ym} = 522 \times 10^{-6}$ ($\sigma_{ym} = 108.0$ MPa). In the last analysed section III-III, the maximum strains (normal stresses) obtained from the calculations in the transversal direction of the shell structure were obtained in the top of corrugations during the compaction of the 20th backfill layer, and their value amounted to $\varepsilon_{yc} = 581 \times 10^{-6}$ ($\sigma_{yc} = 120.3$ MPa). In this case the strain level was $\varepsilon_{ym} = 599 \times 10^{-6}$ ($\sigma_{ym} = 124.0$ MPa) (Fig. 5(b)).

During backfilling and soil compacting, the steel shell structure works in two main phases. The first concerns the shell that is not fully buried yet (Fig. 5(a)), and the second one refers to the shell already buried (Fig. 5(b)). In the first case the total strains and normal stresses are dependent to a greater extent on the bending moments than the axial forces. Whereas, in the second case it is vice versa, i.e., the axial forces have a dominant influence on the level of normal stresses (like in the classical arc, Fig. 8(b)).

5.4 Bending moments

The highest bending moments obtained from the FDM calculations in steel shell structures

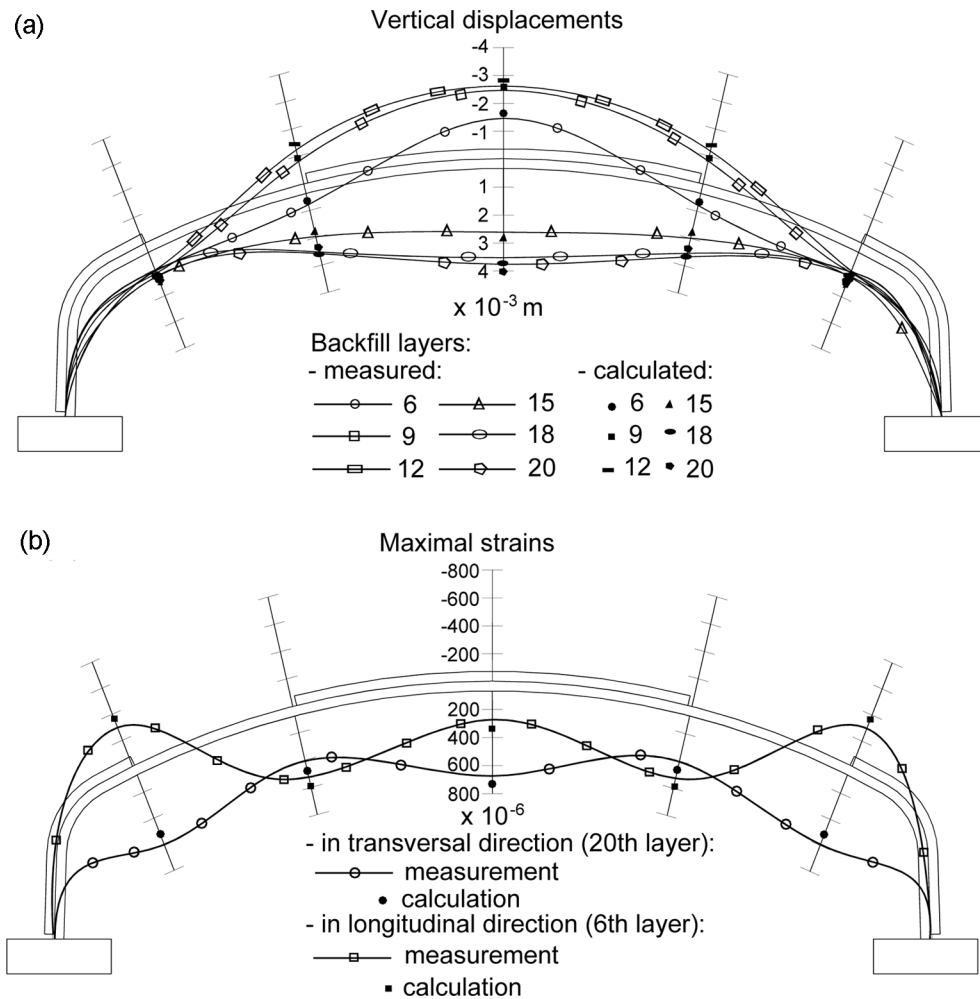


Fig. 8 Comparison of maximum values of vertical displacements (a) and strains (b) in longitudinal direction of structure, received from calculations and tests during backfilling

occurred in section III-III during compaction of the 9 backfill layer, and their maximum value amounted to 247.2 MPa (Fig. 7(a)). In the first section I-I, i.e., in the crown of the shell, the maximum bending moments equalled 159.0 MPa. This occurred during compaction of the 18 backfill layers (Fig. 7(b)). In the last section II-II, the maximal bending moment amounted to 92.6 MPa during compaction of the 20th backfill layer.

6. Conclusions

As a result of the numerical analyses carried out on the corrugated steel plate (CSP) bridge during backfilling process, the vertical displacements, strains (indirectly normal stresses) and bending moments of the load-carrying structure were determined and compared with the measured values

(Figs. 7 and 8). Based on the practical experience gained from a comprehensive analysis (calculations and tests), and the observations concerning the behaviour of the soil-steel bridge, the following general conclusions can be drawn:

1. The average displacement and strain (normal stress) values obtained from the FDM calculations were mostly higher than the field measurements at almost all nodal points under the same loads. The causes of the discrepancy stem mainly from the calculations with the assumed underestimated value of interaction of the shell with the soil and cautious underestimation of the steel shell structure stiffness (in calculations it is assumed that there are not corrugations). The mostly lower average displacement and strain values of the shell obtained from the measurements as compared to the calculated values proves that the cross section has considerably higher rigidity (soil-steel system).
2. As the effect of executed calculations by the FDM and compared with experimental ones affirmed, the two-dimensional 2D analysis of backfilling process is quite sufficient for engineering practice. In some special cases, the three-dimensional model could be executed with the aim of more detailed analysis. It is also important to add that in the case of the three-dimensional analysis, the magnitude of problem increases significantly. Moreover, the process of creating computational models becomes more arduous and quite complicated. The modelling of soil as the Duncan-Chang model (the hyperbolic stress-strain relationship) is recommended. With regard to the steel shell, the typical elements and methods of analysis can be used e.g., bilinear elastic material.
3. The selection of correct interface element properties is very important and crucial to analysis of soil-steel bridges. The contact layers of *interface* type with non-linear properties should be considered between soil and steel elements.
4. The computational examples implemented on the real bridge object and comparison of the calculation results with experimental ones showed that the *FLAC 2D* computer program based on the FDM is a quite good tool permitting the creation of the numerical models of the soil-steel bridge structure. Such analysis can be applied instead of extremely expensive and time-consuming experimental tests being carried out on the individual real objects.
5. It is extremely important in such steel-soil bridge types to provide stability of the steel shell during the construction of its particular elements, especially during the compaction of the backfill around the shell structure. The thin shell structure is very flexible to any loads acting on it (particularly to the lateral soil pressure). During the backfilling process, the CSP shell structure and the soil media do not yet have sufficient interaction; which they will not achieve until after the finishing of the construction works.

References

- AASHTO (2002), *Standard Specifications for Highway Bridges*, American Association of State Highway and Transportation Officials, New York.
- Arockiasamy, M., Chaallal, O. and Limpeteprakarn, T. (2006), "Full-scale field tests on flexible pipes under live load application", *J. Perf. Constr. Fac.*, **20**(1), 21-27.
- Beben, D. (2005), "Soil-structure interaction in bridges made from steel corrugated plates", Ph.D. Thesis, Opole University of Technology, Opole, Poland.
- Beben, D. (2009), "Numerical analysis of a soil-steel bridge structure", *Baltic J. Road and Bridge Eng.*, **4**(1), 13-21.
- Beben, D. and Manko, Z. (2010), "Dynamic testing of a soil-steel bridge", *Struct. Eng. Mech.*, **35**(3), 301-314.
- Cundall, P.A. and Hart, R.D. (1992), "Numerical modeling of discontinua", *Eng. Comput.*, **9**(2), 101-113.

- Dancygier, A.N. and Karinski, Y.S. (2000), "A model to analyze a buried structure response to surface dynamic loading", *Struct. Eng. Mech.*, **9**(1), 69-88.
- Duncan, J.M. and Chang, C.Y. (1970), "Nonlinear analysis of stress and strain in soils", *J. Soil Mech. Found. Div.*, **96**(SM5), 1629-1653.
- El-Sawy, K.M. (2003), "Three-dimensional modeling of soil-steel culverts under the effect of truckloads", *Thin Wall. Struct.*, **41**(8), 747-768.
- Flener, E.B. (2010), "Soil-steel interaction of long-span box culverts – performance during backfilling", *J. Geotech. Geoenviron. Eng.*, **136**(6), 823-832.
- Flener, E.B. and Karoumi, R. (2009), "Dynamic testing of a soil-steel composite railway bridge", *Eng. Struct.*, **31**(12), 2803-2811.
- Flener, E.B., Karoumi, R. and Sundquist, H. (2005), "Field testing of a long-span arch steel culvert during backfilling and in service", *Struct. Infrastruct. Eng.*, **1**(3), 181-188.
- Hernandez-Montes, E., Aschheim, M., and Gil-Martin, L.M. (2005), "The buried arch structural system for underground structures", *Struct. Eng. Mech.*, **20**(1), 69-83.
- Hu, L. and Pu, J.L. (2003), "Application of damage model for soil-structure interface", *Comput. Geotech.*, **30**(2), 165-183.
- Kang, J., Parker, F. and Yoo, Ch. (2008), "Soil-structure interaction for deeply buried corrugated steel pipes. Part I: Embankment installation", *Eng. Struct.*, **30**(2), 384-392.
- Karinski, Y.S., Yankelevsky, D.Z. and Antes, M.Y. (2009), "Stresses around an underground opening with sharp corners due to non-symmetrical surface load", *Struct. Eng. Mech.*, **31**(6), 679-696.
- Kim, K. and Yoo, Ch. (2005), "Design loading for deeply buried box culverts", *J. Geotech. Geoenviron. Eng.*, **131**(1), 7-20.
- Lambe, T.W. (1973), "Predictions in soil engineering", *Geotechnique*, **23**(2), 149-202.
- Ma, G.W., Huang, X. and Li, J.C. (2009), "Damage assessment for buried structures against internal blast load", *Struct. Eng. Mech.*, **32**(2), 301-320.
- Manko, Z. and Beben, D. (2005a), "Research on steel shell of a road bridge made of corrugated plates during backfilling", *J. Bridge Eng.*, **10**(5), 592-603.
- Manko, Z. and Beben, D. (2005b), "Static load tests of a road bridge with a flexible structure made from Super Cor type steel corrugated plates", *J. Bridge Eng.*, **10**(5), 604-621.
- Manko, Z. and Beben, D. (2005c), "Tests during three stages of construction of a road bridge with a flexible load-carrying structure made of Super Cor type steel corrugated plates interacting with soil", *J. Bridge Eng.*, **10**(5), 570-591.
- Manko, Z. and Beben, D. (2008), "Dynamic testing of a corrugated steel arch bridge", *Can. J. Civil Eng.*, **35**(3), 246-257.
- McGrath, T.J., Moore, I.D., Selig, E.T., Webb, M.C. and Taleb, B. (2002), "Recommended specifications for large-span culverts," National Cooperative Highway Research Program Report 473, Transportation Research Board, National Research Council, Washington, D.C.
- Nagy, N., Mohamed, M. and Boot, J.C. (2010), "Nonlinear numerical modelling for the effects of surface explosions on buried reinforced concrete structures", *Geomech. Eng.*, **2**(1), 1-18.
- Petterson, L. and Sundquist, H. (2007), *Design of Soil Steel Composite Bridges*, TRITA-BKN, Third edition, Stockholm.
- Rotter, J.M. and Jumikis, P.T. (1998), *Non-Linear Strain Displacement Relations for Axi-Symmetric Thin Shell*, Research Report R563, School of Civil and Mining Engineering, University of Sydney, New South Wales, Australia.
- Sargand, S., Masada, T. and Moreland, A. (2008), "Measured field performance and computer analysis of large-diameter multiplate steel pipe culvert installed in Ohio", *J. Perf. Constr. Fac.*, **22**(6), 391-397.
- Sezen, H., Yeau, K.Y. and Fox, P.J. (2009), "In-situ load testing of corrugated steel pipe-arch culverts", *J. Perf. Constr. Fac.*, **22**(4), 245-252.
- Vaslestad, J. (1990), "Soil structures interaction of buried culverts", Ph.D. Thesis, Norwegian Institute of Technology, Trondheim, Norway.
- Yeau, K.Y., Sezen, H. and Fox, P.J. (2009), "Load performance of in situ corrugated steel highway culverts", *J. Perf. Constr. Fac.*, **23**(1), 32-39.

- Kunecki, B. (2006), "Full-scale test of corrugated steel culvert and fem analysis with various static systems", *Stud. Geotech. Mech.*, **28**(2-4), 39-54.
- Machelski, Cz. and Antoniszyn, G. (2004), "Influence of live loads on the soil-steel bridges", *Stud. Geotech. Mech.*, **26**(3-4), 91-119.
- Machelski, Cz., Antoniszyn, G. and Michalski, B. (2006), "Live load effects on a soil-steel bridge founded on elastic supports", *Stud. Geotech. Mech.*, **28**(2-4), 65-82.
- Taleb, B. and Moore, I.D. (1999), "Metal culvert response to earth loading. Performance of two-dimensional analysis", Transportation Research Record, No. 1656, *J. Transp. Res. Board*, 25-36.